Nuclear Science and Techniques (2023) 34:108
https://doi.org/10.1007/s41365-023-01256-6

Tandem catalysis for enhanced CO oxidation over the Bi–Au–SiO_2 interface

Huan Zhang[1,2,3] · Lei Xie[2] · Zhao-Feng Liang[2] · Chao-Qin Huang[2,3] · Hong-Bing Wang[2,3] · Jin-Ping Hu[2,3] · Zheng Jiang[2,3] · Fei Song[2,3]

Received: 11 November 2022 / Revised: 31 March 2023 / Accepted: 18 April 2023 / Published online: 24 July 2023

Abstract
Bimetallic catalysts typically exploit unique synergetic effects between two metal species to achieve their catalytic effect. Understanding the mechanism of CO oxidation using hybrid heterogeneous catalysts is important for effective catalyst design and environmental protection. Herein, we report a Bi–Au/SiO_2 tandem bimetallic catalyst for the oxidation of CO over the Au/SiO_2 surface, which was monitored using near-ambient-pressure X-ray photoelectron spectroscopy. The Au-decorated SiO_2 catalyst exhibited scarce activity in the CO oxidation reaction; however, the introduction of Bi to the Au/SiO_2 system promoted the catalytic activity. The mechanism is thought to involve the dissociation O_2 molecules in the presence of Bi, which results in spillover of the O species to adjacent Au atoms, thereby forming $Au^{\delta+}$. Further CO adsorption, followed by thermal treatment, facilitated the oxidation of CO at the Au–Bi interface, resulting in a reversible reversion to the neutral Au valence state. Our work provides insight into the mechanism of CO oxidation on tandem surfaces and will facilitate the rational design of other Au-based catalysts.

Keywords APXPS · CO oxidation · Au–Bi interface · Tandem catalysis · In situ

1 Introduction

The unique synergetic effect between the two metal species in bimetallic catalysts has been studied for decades [1–6]. Active sites with specific geometries can be regulated by the introduction of a second metal via the ensemble effect, which has increased interest in bimetallic catalytic systems in recent years [7–10]. Goodman et al. first demonstrated that numerous factors can significantly affect the catalytic performance of Au catalysts [11, 12], including the addition of a second metal. Bimetallic catalysts based on Au-based bimetallic catalysts (Au–*X*, where *X* = Pd, Ag, Pt, etc.) have emerged as an attractive catalytic system for many reactions, particularly CO oxidation [13–18]. For example, the addition of Pd to Au/SnO_2 and Au/TiO_2 systems enhances their catalytic activity in low-temperature CO oxidation reactions [19, 20]. In such systems, where Au atoms provide active sites for CO adsorption, contiguous Pd sites were responsible for O_2 dissociation [21–23]. Despite the numerous investigations on bimetallic catalysts for CO oxidation published in the last decade, effective advanced bimetallic catalysts and their intrinsic mechanisms and synergetic effects are yet to be discovered and explored.

Bi is commonly used in liquid-phase alcohol generation [23–26] and electrochemical applications [27–29] owing to its low toxicity, low cost, and environmental sustainability. In bimetallic systems, it is generally accepted that Bi exists in a higher oxidation state and prevents the oxidation of

This work was supported by the National Natural Science Foundation of China (Nos.11874380 and 22002183) and the National Key Research and Development Program of China (No. 2021YFA1600800).

✉ Lei Xie
xiel@sari.ac.cn

✉ Fei Song
songfei@sinap.ac.cn

[1] Instrumentation and Service Center for Physical Sciences, Westlake University, Hangzhou 310024, China

[2] Shanghai Synchrotron Radiation Facility, Shanghai Advanced Research Institute, Chinese Academy of Sciences, Shanghai 201204, China

[3] Shanghai Institute of Applied Physics, Chinese Academy of Sciences, Shanghai 201800, China

noble metals [30–34]. We previously demonstrated that the Bi–Cu interface exhibited higher catalytic activity for CO_2 activation and dissociation than pure Cu(111). The introduction of Bi atoms causes the dissociated O to migrate to the Cu–Bi sites, thereby freeing the Cu active sites at which CO_2 dissociation occurs and thus boosting the catalytic activity [35]. Nan et al. recently reported the enhanced catalytic activity of Pt–Bi catalysts for CO oxidation [36], in which the unique Pt–Bi interfaces provided superior activation of oxygen species at low temperatures and increased CO_2 production. An Au–Bi catalyst exhibited an interesting phenomenon during the hydrochlorination of acetylene, where electron transfer between Au and Bi led to the dispersion of Au nanoparticles in a higher valence state, which enhanced C_2H_2 absorption [37]. Based on these previous results, we decided to investigate whether similar effects could be achieved by the addition of Bi to Au-based catalysts for other typical catalytic reactions.

Recent advances in in situ characterization have enabled the exploration of surface segregation and reductive/oxidative evolution of model catalysts under near-ambient pressures. For example, near-ambient-pressure X-ray photoelectron spectroscopy (NAP-XPS) is a powerful tool for elucidating reaction mechanisms because changes in the core-level orbitals of each reactant can be measured directly over the course of the reaction. Herein, NAP-XPS was employed to investigate the role of Bi in improving the catalytic performance of the Au–Bi/SiO_2 surface for CO oxidation. To achieve this goal, the catalytic activities of Au/SiO_2, Bi/SiO_2, and Au–Bi/SiO_2 catalysts with different coverages were evaluated using several separate in situ experiments. The Au 4f peaks in the NAP-XPS spectra of Au/SiO_2 catalysts did not significantly change during reactions under at both oxidative and reductive conditions, while the Bi sites in Au–Bi/SiO_2 facilitated the contiguous dissociation of O_2 with a further spillover of O species to Au, thus forming $Au^{\delta+}$. Furthermore, strong interactions between Bi and CO were identified. Meanwhile, a reversible shift of the Au 4f peaks was observed, indicating the reversion of $Au^{\delta+}$ to metallic Au, thus confirming the catalytic activity of Au–Bi surfaces in CO oxidation under the employed reaction conditions. This study illustrates the syntactic activity for CO oxidation of a Au–Bi/SiO_2 tandem surface in CO oxidation, which may facilitate the design of bimetallic catalysts containing Au species.

2 Materials and methods

This study was conducted using Beamline 20U at the Shanghai Synchrotron Radiation Facility (SSRF). All NAP-XPS spectra were recorded with a Hipp-2 analyzer (Scienta Omicron) with a monochromated Al Kα radiation source ($h\nu = 1486.6$ eV, SPECS) [38]. The ultrahigh vacuum (UHV) system was equipped with analysis and preparation chambers, with base pressures of 7×10^{-10} mbar and 5×10^{-10} mbar, respectively. The SiO_2 substrate (MaTeck) was mounted on a Ta sample holder and heated via laser heating from the rear. The surface was cleaned by repeated annealing at 1000 K in UHV until C species were no longer detected by C 1s XPS. The gas pipelines were purified using a mixture of alcohol and liquid nitrogen at approximately 173 K and monitored in situ using mass spectrometry to ensure no additional gas cross-contamination. The dosing gases were introduced into the analysis chamber using a leak valve and were equilibrated for at least 30 min prior to analysis. The XPS spectra were fitted with Gaussian–Lorentz peaks [39] using Casa XPS software after subtraction of the Shirley background.

3 Results

The catalytic activities of Au/SiO_2, Bi/SiO_2, and bimetallic Au–Bi/SiO_2 in the oxidation of CO were compared by exposing these samples to O_2 and CO atmospheres. The Au 4f and O1s XPS spectra of a 0.4 monolayer (ML) Au/SiO_2 sample are shown in Fig. 1. The photoelectron spectra were recorded in the presence of O_2 (0.1 mbar) from room temperature (RT) to 373 K and separately in the presence of CO (0.1 mbar) atmosphere from RT to 473 K. The Au 4f spectrum obtained prior to any catalytic reactions shows peaks corresponding to metallic Au at 84.0 eV (Au 4f7/2) and 87.7 eV (Au 4f5/2), demonstrating that only standard metallic Au species are present. Under these conditions, a single O peak characteristic of the SiO_2 substrate was observed at 531.7 eV. The shape and position of the Au 4f spectra remained essentially unchanged during the O_2/CO switching exposure process (Fig. 1a), indicating preservation of the metallic Au species. Upon exposure to O_2 (0.1 mbar) at RT, a peak at 531.7 eV (O_I) is observed, which increases slightly at 373 K, and thereafter remains essentially unchanged with increasing temperature (Fig. 1b). Greg et al. reported that the highest occupied molecular orbital (HOMO) in Au clusters and rough Au surfaces is localized, and its charge density distribution facilitates charge transfer into the π* orbital of O_2, which induces the binding of the molecule to gold. The HOMO of a flat face of a bulk surface tends be delocalized, which diminishes the ability of the surface to bind O_2 [40]. Conversely, the oxidation of the Au(111) surface increases with temperature [41], contrary to the results depicted in Fig. 1. The Au 4f peak (Fig. 1a) does not indicate the oxidation of Au; thus, we attributed the O_I component to the chemisorption of O_2 molecules on the Au species. At 373 K, the O_2 coverage of the surface, which is reflected by the peak intensity, approached the relative maximum. The intensity

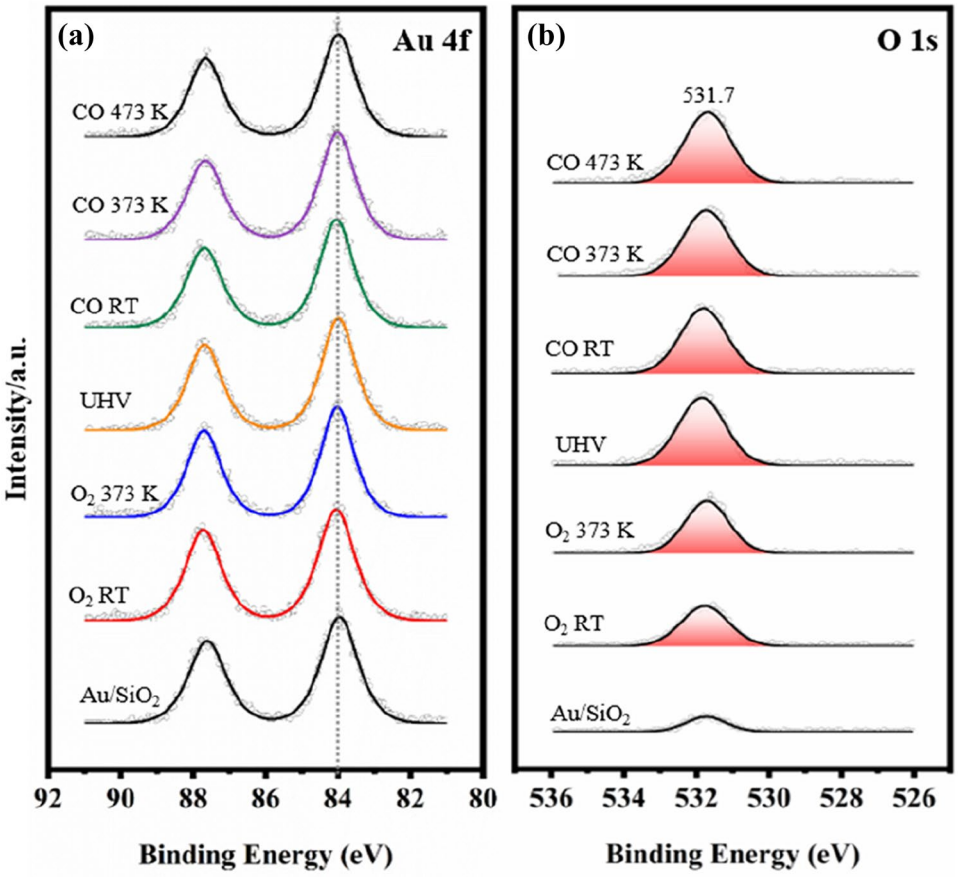

Fig. 1 (Color online) In situ O_2/CO switching measurements on the Au/SiO_2 surface. **a** Au 4f and **b** O 1 s spectra recorded after exposure to O_2 (0.1 mbar) and CO (01 mbar) under various experimental conditions

of the peak corresponding to O increased after dosing with CO (Fig. 1b, upper part), indicating CO adsorption on the surface at the same binding energy (BE). Metallic Au exhibits poor CO adsorption activity because adsorption requires negatively charged Au atoms, which are formed by back donation from the Au d-electrons to the antibonding π* orbital of the adsorbed CO molecules [42–44]. Thus, CO is most likely adsorbed on the SiO_2 surface in this case, as Au remains in the inert metallic state (Fig. S1). No BE shift of the Au 4f peaks was observed upon the adsorption of gas molecule, which was attributed to following reason: the sample surface exhibits poor activity under the experimental conditions, causing the concentration of adsorbed gas phase molecules is below the detection limit.

Considering the role of bismuth in promoting the catalytic activity of bimetallic catalysts [35], in situ AP-XPS spectra of the Bi/SiO_2 samples were also obtained to elucidate the effect of the O_2/CO atmosphere and annealing temperature (Fig. 2). To obtain a dense Bi surface, multiple layers of Bi were deposited on SiO_2 via vacuum sublimation of the Bi powder, followed by thermal annealing at 473 K to ensure a uniform distribution. The Bi 4f spectrum obtained under UHV at RT presents peaks characteristic of metallic Bi at 157.0 eV (Bi 4f7/2) and 162.3 eV (Bi 4f5/2). After introducing 0.1 mbar O_2 to the system at RT, immediate changes were found in the Bi 4f spectrum, where the pristine metallic Bi component was weakened, along with new sharp peaks appearing at 159.0 eV and 162.3 eV, respectively, suggesting the formation of the bismuth oxidation state ($Bi^{\delta+}$) [45]. In addition to the O_I component, another peak corresponding O emerges at 529.7 eV (Fig. 2b), which was assigned to oxygen–metal (O–M) bonding (denoted as O_{II}) [46]. Thus, in this case, Bi–O bonding was induced by O species originating from O_2 dissociation [47, 48]. In addition, the O 1s peak with a higher BE at 531.7 eV (the same BE as the adsorption of O_2 on SiO_2, Fig. 1) arises from the bonding between Bi and absorbed O_2 [48].

After evacuating the chamber to UHV and subsequently introducing CO (0.1 mbar) at RT, the signal corresponding metallic Bi (green shadow) is reduced in intensity, demonstrating the further oxidation of Bi. This behavior is similar to that observed under an O_2 atmosphere and may result from the adsorption of CO and further dissociation on Bi/SiO_2 surface. To prove this hypothesis, a control experiment was conducted in which Bi/SiO_2 was directly exposed to CO (Fig. S2a and S2b). Similarly, CO adsorption resulted in the oxidation of Bi at RT, and the degree of oxidation increased with temperature, as reflected by the both the O_I (Bi–CO in

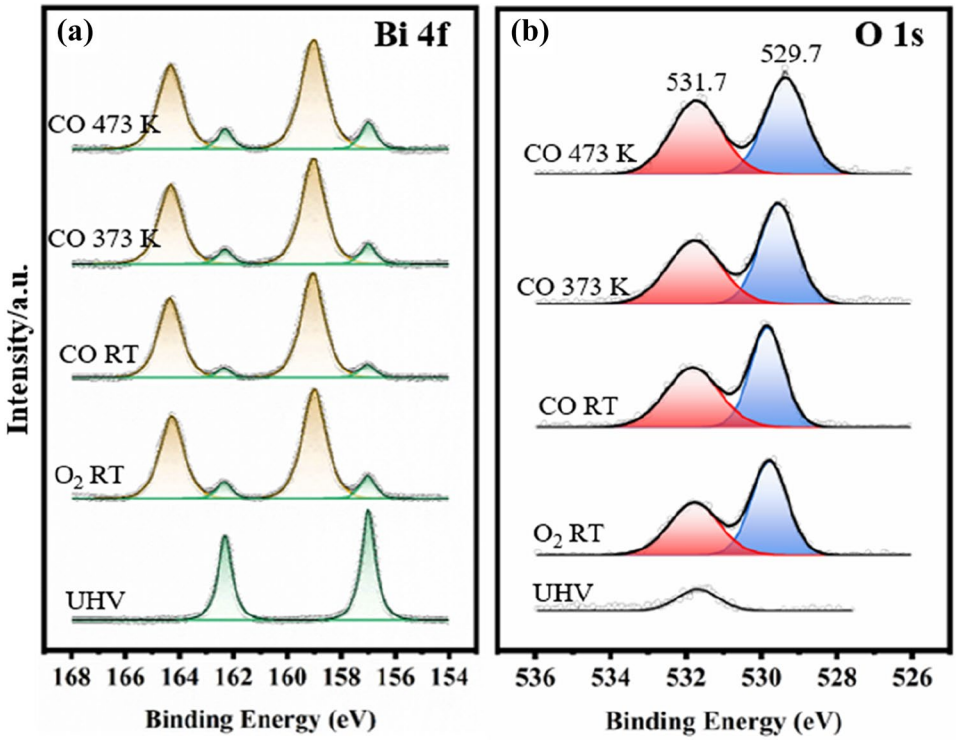

Fig. 2 (Color online) In situ XPS **a** Bi 4f and **b** O 1 s spectra of the Bi/SiO_2 surface in O_2/CO atmospheres under various experimental conditions

red) and O_{II} (Bi–O in blue) components in the Bi 4f and O 1s spectra. This oxidized state is rather stable, and the Bi 4f and O 1s spectra remain essentially unchanged upon further introduction of a 0.1 mbar H_2 reductive atmosphere followed by annealing (Fig. S2c and S2d). Thus, we conclude that the weakened metallic Bi component in the spectra after the introduction of CO at RT (Fig. 2a) originates from CO adsorption and dissociation. After further thermal treatment, the intensity of the peak corresponding to f metallic Bi increased with temperature from 373 to 473 K (Fig. 2a) owing to the reduction in the oxidative surface. This may be explained by the oxidation of CO by the O species adsorbed on the surface, resulting in the formation of the CO_2 product. Without O_2 pretreatment, the Bi/SiO_2 surface underwent a continuous oxidation process, and the reduction reaction that prevailed after annealing in a CO atmosphere did not occur.

To explore the CO oxidation reaction on the bimetallic surface, a $Au–Bi/SiO_2$ sample was prepared by depositing 0.4 ML Au particles on a Bi/SiO_2 surface. The XPS spectra of the bimetallic surface are shown in Fig. 3. In contrast with the spectra of the Au/SiO_2 sample during O_2 exposure, wherein Au maintained a metallic state (Fig. 1), the Au 4f peaks in spectrum of the bimetallic sample shift upwards by 0.2 eV (4f5/2 at 87.9 eV and 4f7/2 at 84.2 eV) relative to the metallic Au peak in the presence of O_2 (0.1 mbar) at RT (Fig. 3a), indicating the existence of $Au^{\delta+}$, which did not appear in the absence of Bi under equivalent experimental conditions. The formation of a Au–Bi alloy, which can also result in a Au BE shift [6], can be excluded in this case as the Au BE in the spectrum of another sample of $Au–Bi/SiO_2$ remains unchanged under a CO atmosphere (Fig. S3). Therefore, the upward shift in the Au BE was reliably attributed to the Au oxidation state.

Similarly, $Bi^{\delta+}$ is also formed upon introduction of O_2, with Bi 4f peaks appearing at 159.0 eV and 162.3 eV (Fig. 3b), indicating the oxidation of Bi. Similarly, the O 1s peak located at a BE of 529.7 eV (Fig. 3c) increased compared with that observed at UHV, providing evidence of O_2 dissociation and the formation of O–M bonds. Similarly, the component at 531.7 eV (Fig. 3c) arising from O_2 adsorption on the surface also increases. Considering the strong role of adjacent Bi atoms in the capture and decomposition of O_2 molecules (Fig. 2), we concluded that the upward shift of the Au BE was caused by the migration of adsorbed O atoms (originating from O_2 dissociation) from the contiguous Bi sites. This conclusion is also consistent with Goodman's mechanism [15, 16], which suggests that O_2 dissociation occurs at the contiguous metal sites with further spillover of the adsorbed O species to Au atoms, which allows further CO oxidation. After annealing at 373 K, the fraction of metallic Bi was reduced, and the intensity of the two signals in the O 1s region increased, suggesting that the surface has a higher oxidation state owing to the intensification of the oxidation reaction.

After the addition CO gas followed by annealing to 473 K, the fraction of metallic bismuth was strengthened

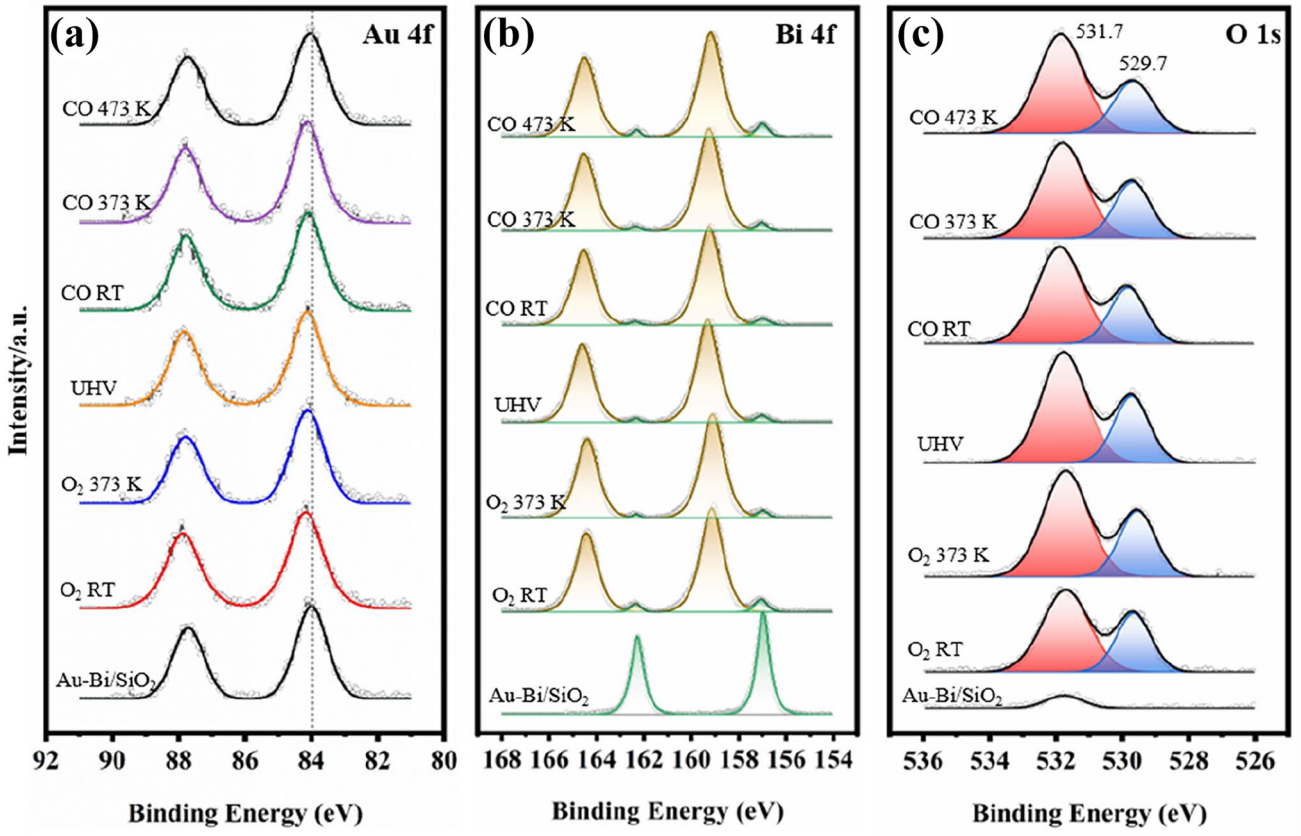

Fig. 3 (Color online) **a** Au 4f and **b** Bi 4f and **c** O 1 s spectra of Au–Bi/SiO_2 under O_2/CO atmospheres under various experimental conditions. O_2 and CO were present at a pressure of 0.1 mbar. The bottom spectra (labeled "Au–Bi/SiO_2") were obtained under UHV

(upper part of Fig. 3b, the intensity ratio evolution of $Bi^{\delta+}$/Si 2p is given in Fig. S4), which agrees with the phenomenon exhibited by the Bi/SiO_2 sample, in which the CO oxidation reaction occurs at the Bi sites. After annealing, the total amount of the O component decreased (Fig. 3c and Fig. S4), suggesting that the CO molecules reduced the surface oxides (Fig. 3c). Additionally, the Au 4f peak shifts returns to its original position under UHV (Fig. 3a) after annealing at 473 K in a CO atmosphere, indicating that $Au^{\delta+}$ is reduced to metallic Au. Thus, we achieved reversible alternation of the Au state in oxidizing and reducing atmospheres by adding Bi to the Au/SiO_2 system. The XPS analysis shows the enhanced catalytic activity of the Bi–Au–SiO_2 interface in the oxidation of CO, relative to the case in Fig. 1. The universality of this phenomenon is further verified in Fig. S5 with lower Au coverage.

To clearly demonstrate the mechanism of the CO oxidation reaction on different samples, models illustrating the proposed mechanism are shown in Fig. 4. The original Au/SiO_2 surface was essentially inactive during both O_2 dissociation and CO adsorption, thereby blocking further reactions (Fig. 4a). The Bi/SiO_2 catalyst exhibited some activity for the CO oxidation reaction owing to the strong CO adsorption capacity and O_2 dissociation ability of Bi (process IV in Fig. 4b). The reversible shift of the Au 4f peaks in the spectrum of the Au–Bi/SiO_2 sample suggests that CO oxidation was indeed activated by the bimetallic surface. Based on these observations, a mechanism of CO oxidation on the Au–Bi/SiO_2 surface can be proposed (Fig. 4c). After exposure to O_2, the rapidly dissociated oxygen species on the Bi sites migrate to the neighboring Au atoms and form Au–O bonds (process III). The relatively strong interaction between Bi and CO enabled the surface to capture CO molecules (process IV); thus, the combination of adsorbed CO and O on both the Bi and Au sites occurred simultaneously with desorption of the CO_2 product from the surface (process V), resulting in the recovery of the Au valence state. The Au and Bi species, indicated by orange and dark blue spheres in Fig. 4, may be atoms or clusters. Thus, adjacent Bi sites facilitated the adsorption of O_2 and CO molecules on Au/SiO_2, and the tandem surface catalyzed the CO oxidation reaction. Because bismuth species are partly oxidized in O_2 at RT (Fig. 2a and Fig. 3b), the subsequent upshift in the Au BE observed under a CO atmosphere may be a consequence of Au–BiO_x formation and the enhanced catalytic activity of the interface. We also considered changing the sequence

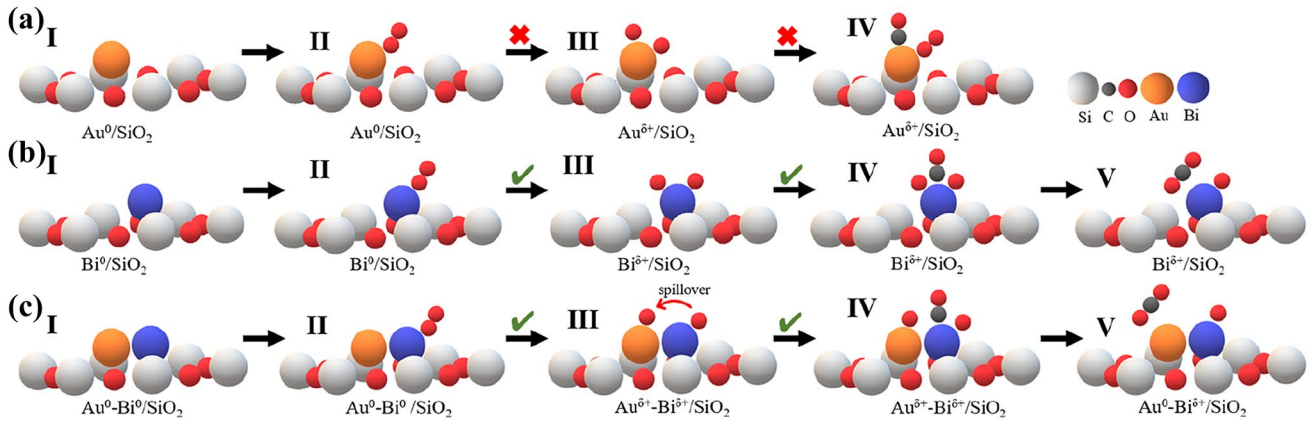

Fig. 4 (Color online) Schematic of the proposed mechanism of CO oxidation on the surface of **a** Au/SiO_2 **b** Bi/SiO_2, and **c** $Au-Bi/SiO_2$ catalysts. I Fresh sample surface. II Generation of $Bi^{\delta+}$ after O_2 adsorption. III (b) Dissociation of O_2 molecules on Bi. (c) Oxidation of Au owing to spillover of adsorbed O from neighboring Bi sites. IV Bi-CO bonding resulting from strong adsorption. V Generation of CO_2 from adsorbed CO and O, (c) neutralization of Au and recovery of the catalyst

of introduced gas to explore the $Au–BiO_x$ interface and CO adsorption state on the sample surface because the Bi atoms sites may be permanently occupied by the adsorption of CO molecules, in which case no distinct difference in the chemical states of Bi would be distinguishable during subsequent processes. Therefore, NAP-XPS alone may not be sufficient to elucidate the role of the Au–BiO interface in enhancing the activity of the catalyst. Additional characterization methods may be required to provide a deeper insight into the role of the interface.

4 Conclusion

AP-XPS was employed to investigate the surface evolution of $Au–Bi/SiO_2$ tandem catalysts for CO oxidation and to elucidate the origin of the enhanced catalytic activity. O_2 dissociation and CO adsorption do not readily occur on the Au particles adsorbed on the SiO_2 substrate; accordingly, the CO oxidation reaction was highly suppressed. Conversely, the introduction of Bi improves the O_2 dissociation ability of the surface, and the adsorbed O atoms subsequently spill over to adjacent Au atoms, resulting in the formation of $Au^{\delta+}$. Further CO adsorption on Bi, followed by thermal treatment, facilitated the CO oxidation reaction at the Au–Bi interface, resulting in a reversible shift of the Au valence state to neutral. This study illustrates that the performance of Au/SiO_2 catalysts can be manipulated by Bi doping, which will shed new light on the design of bimetallic catalysts containing inert Au species.

Supplementary Information The online version contains supplementary material available at https://doi.org/10.1007/s41365-023-01256-6.

Author contributions All authors contributed to the study conception and design. Material preparation, data collection, and analysis were performed by Huan Zhang, Zhao-Feng Liang, and Lei Xie. The first draft of the manuscript was written by Huan Zhang, and all authors commented on previous versions of the manuscript. All authors read and approved the final manuscript.

Data availability The data that support the findings of this study are openly available in Science Data Bank at https://www.doi.org/10.57760/sciencedb.08938 and https://cstr.cn/31253.11.sciencedb.08938.

Declarations

Conflict of interest Fei Song is an editorial board member for *Nuclear Science and Techniques* and was not involved in the editorial review, or the decision to publish this article. All authors declare that there are no competing interests.

References

1. C. Wu, C. Liu, D. Su et al., Bimetallic synergy in cobalt–palladium nanocatalysts for CO oxidation. Nat. Catal. **2**, 78–85 (2019). https://doi.org/10.1038/s41929-018-0190-6
2. D. Kim, J. Resasco, Y. Yu et al., Synergistic geometric and electronic effects for electrochemical reduction of carbon dioxide using gold–copper bimetallic nanoparticles. Nat. Commun. **5**, 4948 (2014). https://doi.org/10.1038/ncomms5948(2014)
3. J.L. Snider, V. Streibel, M.A. Hubert et al., Revealing the synergy between oxide and alloy phases on the performance of bimetallic In-Pd catalysts for CO_2 hydrogenation to methanol. ACS Catal. **9**, 3399–3412 (2019). https://doi.org/10.1021/acscatal.8b04848
4. M. Khanuja, B.R. Mehta, S.M. Shivaprasad, Geometric and electronic changes during interface alloy formation in Cu/Pd bimetal layers. Thin Solid Films **516**, 5435–5439 (2008). https://doi.org/10.1016/j.tsf.2007.07.117
5. J.A. Rodriguez, D.W. Goodman, The nature of the metal–metal bond in bimetallic surfaces. Science **257**, 897–903 (1992). https://doi.org/10.1126/science.257.5072.897

6. H.S. Yu, X.J. Wei, J. Li et al., The XAFS beamline of SSRF. Nucl. Sci. Tech. **26**(06), 6–12 (2015). https://doi.org/10.13538/j.1001-8042/nst.26.050102
7. A.V. Bukhtiyarov, I.P. Prosvirin, A.A. Saraev et al., In situ formation of the active sites in Pd–Au bimetallic nanocatalysts for CO oxidation: NAP (near ambient pressure) XPS and MS study. Faraday Discuss. **208**, 255 (2018). https://doi.org/10.1039/c7fd00219j
8. M.A. Languille, E. Ehret, H.C. Lee et al., In-situ surface analysis of AuPd(110) under elevated pressure of CO. Catal. Today **260**, 39–45 (2016). https://doi.org/10.1016/j.cattod.2015.05.029
9. L. Delannoy, S. Giorgio, J.G. Mattei et al., Surface segregation of Pd from TiO_2-supported AuPd nanoalloys under CO oxidation conditions observed in situ by ETEM and DRIFTS. ChemCatChem **5**, 2707–2716 (2013). https://doi.org/10.1002/cctc.201200618
10. P.S. West, R.L. Johnston, G. Barcaro et al., The effect of CO and H chemisorption on the chemical ordering of bimetallic clusters. J. Phys. Chem. C **114**, 19678–19686 (2010). https://doi.org/10.1021/jp108387x
11. M. Valden, S. Pak, X. Lai, D.W. Goodman, Structure sensitivity of CO oxidation over model Au/TiO_2 catalysts. Catal, Lett. **56**, 7–10 (1998). https://doi.org/10.1023/A:1019028205985
12. F. Yang, M.S. Chen, D.W. Goodman, Sintering of Au particles supported on TiO_2(110) during CO oxidation. J. Phys. Chem. C **113**, 254–260 (2009). https://doi.org/10.1021/jp807865w
13. W. He, X. Han, H. Jia et al., AuPt alloy nanostructures with tunable composition and enzyme-like activities for colorimetric detection of bisulfide. Sci. Rep. **7**, 40103 (2017). https://doi.org/10.1038/srep40103(2017)
14. B. Zhu, G. Thrimurthulu, L. Delannoy et al., Evidence of Pd segregation and stabilization at edges of AuPd nano-clusters in the presence of CO: a combined DFT and DRIFTS study. J. Catal. **308**, 272–281 (2013). https://doi.org/10.1016/j.jcat.2013.08.022
15. W. Zhan, J. Wang, H. Wang et al., Crystal structural effect of AuCu alloy nanoparticles on catalytic CO oxidation. J. Am. Chem. Soc. **139**, 8846–8854 (2017). https://doi.org/10.1021/jacs.7b01784
16. X. Wei, C. Xiao, K. Wang, Y. Tu, A nano-TiO_2 supported AuAg alloy nanocluster functionalized electrode for sensitizing the electrochemiluminescent analysis. J. Electroanal. Chem. **702**, 37–44 (2013). https://doi.org/10.1016/j.jelechem.2013.05.009
17. Y.H. Lv, Y.H. Zhang, J. Zhang, B. Li, Mössbauer spectroscopy studies on the particle size distribution effect of Fe–B–P amorphous alloy on the microwave absorption properties. Nucl. Sci. Tech. **31**, 24 (2020). https://doi.org/10.1007/s41365-020-0734-8
18. G. Darabdhara, M.R. Das, M.A. Amin et al., Au–Ni alloy nanoparticles supported on reduced graphene oxide as highly efficient electrocatalysts for hydrogen evolution and oxygen reduction reactions. Int. J. Hydrog. **43**, 1424–1438 (2018). https://doi.org/10.1016/j.ijhydene.2017.11.048
19. Q. Ye, J.A. Wang, J.S. Zhao et al., Pt or Pd-doped Au/SnO_2 catalysts: high activity for low-temperature CO oxidation. Catal. Lett. **138**, 56–61 (2010). https://doi.org/10.1007/s10562-010-0360-x
20. T. Ward, L. Delannoy, R. Hahn et al., Effects of Pd on catalysis by Au: CO adsorption, CO oxidation, and cyclohexene hydrogenation by supported Au and Pd−Au catalysts. ACS Catal. **3**, 2644–2653 (2013). https://doi.org/10.1021/cs400569v
21. F. Gao, Y.L. Wang, D.W. Goodman, CO oxidation over AuPd(100) from ultrahigh vacuum to near-atmospheric pressures: the critical role of contiguous Pd atoms. J. Am. Chem. Soc. **131**, 5734–5735 (2009). https://doi.org/10.1021/ja9008437
22. F. Gao, Y.L. Wang, D.W. Goodman, CO oxidation over AuPd(100) from ultrahigh vacuum to near-atmospheric pressures: CO adsorption-induced surface segregation and reaction kinetics. J. Phys. Chem. C **113**, 14993–15000 (2009). https://doi.org/10.1021/ja9008437
23. T. Mallat, Z. Bodnar, C. Bronnimann, A. Baiker, Platinum-catalyzed oxidation of alcohols in aqueous solutions. the role of Bi-promotion in suppression of catalyst deactivation. Stud. Surf. Sci. Catal. **88**, 385–392 (1994). https://doi.org/10.1016/S0167-2991(08)62764-0
24. Y. Miao, Z. Yang, X. Liu et al., Self-assembly of BiIII ultrathin layer on Pt surface for non-enzymatic glucose sensing. Electrochim. Acta **111**, 621–626 (2013). https://doi.org/10.1016/j.electacta.2013.07.188
25. X. Ning, L. Zhan, H. Wang et al., Deactivation and regeneration of in situ formed bismuth-promoted platinum catalyst for the selective oxidation of glycerol to dihydroxyacetone. New J. Chem. **42**, 18837 (2018). https://doi.org/10.1039/c8nj04513e
26. M. Wenkin, P. Ruiz, B. Delmon et al., The role of bismuth as promoter in Pd−Bi catalysts for the selective oxidation of glucose to gluconate. J. Mol. Catal. A Chem. **180**, 141–159 (2002). https://doi.org/10.1016/S1381-1169(01)00421-6
27. L. Peng, Y. Wang, Y. Wang et al., Separated growth of Bi–Cu bimetallic electrocatalysts on defective copper foam for highly converting CO_2 to formate with alkaline anion-exchange membrane beyond $KHCO_3$ electrolyte. Appl. Catal. B: Environ. **288**, 20003 (2021). https://doi.org/10.1016/j.apcatb.2021.120003
28. L. Li, F. Cai, F. Qi, D.K. Ma, Cu nanowire bridged Bi nanosheet arrays for efficient electrochemical CO_2 reduction toward formate. J. Alloys Compd. **841**, 155789 (2020). https://doi.org/10.1016/j.jallcom.2020.155789
29. L. Jia, H. Yang, J. Deng et al., Copper–bismuth bimetallic microspheres for selective electrocatalytic reduction of CO_2 to formate. Chin. J. Chem. **37**, 497–500 (2019). https://doi.org/10.1002/cjoc.201900010
30. T. Mallat, A. Baiker, Oxidation of alcohols with molecular oxygen on platinum metal catalysts in aqueous solutions. Catal. Today **19**, 247–283 (1994). https://doi.org/10.1016/0920-5861(94)80187-8
31. Y. Xiao, J. Greeley, A. Varma et al., An experimental and theoretical study of glycerol oxidation to 1,3-Dihydroxyacetone over bimetallic Pt–Bi catalysts. AIChE J. **63**, 705–715 (2017). https://doi.org/10.1002/aic.15418
32. K. Roy, L. Artiglia, Y. Xiao et al., Role of bismuth in the stability of Pt−Bi bimetallic catalyst for methane mediated deoxygenation of guaiacol, an APXPS study. ACS Catal. **9**, 3694–3699 (2019). https://doi.org/10.1021/acscatal.8b04699
33. H. Guo, H. Yin, X. Yan et al., Pt–Bi decorated nanoporous gold for high performance direct glucose fuel cell. Sci. Rep. **6**, 39162 (2016). https://doi.org/10.1038/srep39162
34. D. Basu, S. Basu, Synthesis, characterization and application of platinum based bi-metallic catalysts for direct glucose alkaline fuel cell. Electrochim. Electrochim. Acta **56**, 6106–6113 (2011). https://doi.org/10.1016/j.electacta.2011.04.072
35. H. Zhang, Z. Liang, C. Huang et al., Enhanced dissociation activation of CO_2 on the Bi/Cu(111) interface by the synergistic effect. J. Catal. **410**, 1–9 (2022). https://doi.org/10.1016/j.jcat.2022.04.001
36. B. Nan, Q. Fu, J. Yu et al., Unique structure of active platinum–bismuth site for oxidation of carbon monoxide. Nat. Commun. **12**, 3342 (2021). https://doi.org/10.1038/s41467-021-23696-7
37. K. Zhou, W. Wang, Z. Zhao et al., Synergistic gold−bismuth catalysis for non-mercury hydrochlorination of acetylene to vinyl chloride monomer. ACS Catal. **4**, 3112–3116 (2014). https://doi.org/10.1021/cs500530f
38. H. Zhang, L. Xie, C.Q. Huang et al., Exploring the CO_2 reduction reaction mechanism on Pt/TiO_2 with the ambient-pressure X-ray photoelectron spectroscopy. Appl. Surf. Sci. **568**, 150933 (2021). https://doi.org/10.1016/j.apsusc.2021.150933

39. M.D. Strømsheim, J. Knudsen, M.H. Farstad et al., Near ambient pressure XPS investigation of CO oxidation over $Pd_3Au(100)$. J. Phys. Chem. C **122**, 21484–21492 (2018). https://doi.org/10.1007/s11244-017-0831-z
40. G. Mills, M.S. Gordon, H. Meitu, Oxygen adsorption on Au clusters and a rough Au(111) surface: the role of surface flatness, electron confinement, excess electrons, and band gap. J. Chem. Phys. **118**, 4198–4205 (2003). https://doi.org/10.1063/1.1542879
41. A.Y. Klyushin, T.C.R. Rocha, M. Hävecker et al., A near ambient pressure XPS study of Au oxidation. Phys. Chem. Chem. Phys. **16**, 7881 (2014). https://doi.org/10.1039/c4cp00308j
42. J.P. Simonovis, A. Hunt, R.M. Palomino et al., Enhanced stability of Pt–Cu single-atom alloy catalysts: in situ characterization of the Pt/Cu(111) surface in an ambient pressure of CO. J. Am. Chem. Soc. **125**, 10437 (2003). https://doi.org/10.1021/acs.jpcc.8b00078
43. D. Stolcic, M. Fischer, G. Ganteför et al., Direct observation of key reaction intermediates on gold clusters. J. Am. Chem. Soc. **125**, 2848 (2003). https://doi.org/10.1021/ja0293406
44. H. Tang, Y. Su, B. Zhang et al., Classical strong metal-support interactions between gold nanoparticles and titanium dioxide. Sci. Adv. **3**, 1700231 (2017). https://doi.org/10.1126/sciadv.1700231
45. B. Afsin, M.W. Roberts, Formation of an oxy-chloride overlayer at a Bi(0001) surface. Spectrosc. Lett. **27**, 139–146 (1994). https://doi.org/10.1080/00387019408002513
46. S. Röhe, K. Frank, A. Schaefer et al., CO oxidation on nanoporous gold: a combined TPD and XPS study of active catalysts. Surf. Sci. **609**, 106–112 (2013). https://doi.org/10.1016/j.susc.2012.11.011
47. M.D. Strømsheim, J. Knudsen, M.H. Farstad et al., Near ambient pressure XPS investigation of CO oxidation over $Pd_3Au(100)$. Top Catal **60**, 1439–1448 (2017). https://doi.org/10.1007/s11244-017-0831-z
48. J.P. Simonovis, A. Hunt, R.M. Palomino et al., Enhanced stability of Pt–Cu single-atom alloy catalysts: in situ characterization of the Pt/Cu(111) surface in an ambient pressure of CO. J. Phys. Chem. C **122**, 4488–4495 (2018). https://doi.org/10.1021/acs.jpcc.8b00078